PERGAMON

International Journal of Multiphase Flow 27 (2001) 1789–1802

International Journal of Multiphase Flow

www.elsevier.com/locate/ijmulflow

Two-phase flow structure near a heated vertical wall during nucleate pool boiling

J. Bonjour, M. Lallemand *

INSA, CETHIL, UMR CNRS 5008, 20, Av. Albert Einstein, 69621 Villeurbanne Cedex, France

Received 23 November 1999; received in revised form 29 March 2001

Abstract

An experimental study has been carried out in order to investigate the two-phase flow structure in the vicinity of a vertical heated wall (120 mm high) on which boiling of pentane takes place. Measurements of the frequency and time of bubble passages and also of void fraction have been performed by means of hot-wire anemometry (HWA). It has been shown that, at high heat flux, bubbles mainly remain close to the wall and form large coalesced bubbles. On the contrary, at low or moderate heat flux, they are propelled into the fluid core prior to rising in a bubble column located about 1.5–2 mm away from the heated wall and sometimes they coalesce during their rising motion in the upper part of the column. Using a classification of bubbles based on their passage time, the contribution from short, average and long bubbles to the void fraction was also discussed. This classification allows to determine the transition between the boiling two-phase flow patterns defined previously from objective criteria: the regime of *isolated bubbles* or *partial nucleate boiling* occurs for $q'/q'_{crit} < 0.2$, the *fully developed nucleate boiling* for $0.2 < q'/q'_{crit} < 0.7$ and the *transition to critical heat flux* (CHF) for $q'/q'_{crit} > 0.7$.

Keywords: Pool boiling; Hot-wire anemometry; Void fraction; Bubble detachment; Bubble motion

1. Introduction

Boiling has been widely developed to replace forced or natural convection for thermal applications such as electronics cooling. That is the reason why this heat transfer mode has been studied extensively during recent years. Therefore, it is of great importance to have a detailed knowledge of the two-phase structure during pool boiling.

* Corresponding author. Tel.: +33-4-72-43-81-54; fax: +33-4-72-43-60-10.
E-mail address: m.lal@cethil.insa-lyon.fr (M. Lallemand).

0301-9322/01/$ - see front matter
PII: S0301-9322(01)00028-3

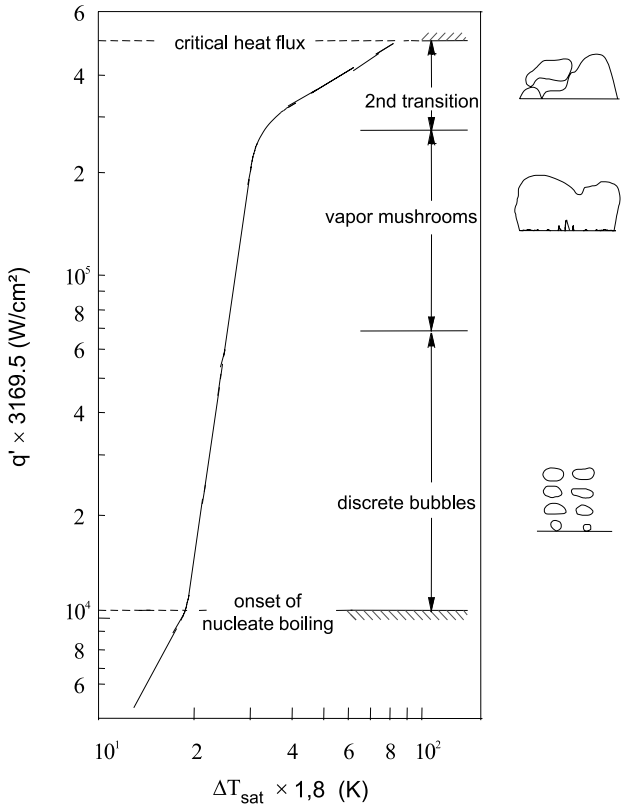

Fig. 1. Boiling curve and regimes observed by Gaertner (1965).

Gaertner (1965) observed three regimes (Fig. 1) during boiling of water on a horizontal copper disk, owing to a photographic study. The regime obtained at low heat flux is called *discrete bubbles*. It is characterised by bubbles that do not interact the ones with the others and that rise up to the free liquid–vapour interface, inducing a moderate agitation of the pool. For a higher heat flux, the regime is called *vapour mushrooms*. Neighbouring bubbles coalesce to form mushroom-shaped large masses of vapour attached to the wall by several stems. The liquid macrolayer between the stems is vapourised during the growth of the mushrooms and allows a high heat transfer coefficient. At very high heat flux occurs the *transition to the critical heat flux* (CHF) also called *second transition* or *vicinity of CHF*, resulting in a change in the slope of the boiling curve. The vapour patches are similar to those observed during the mushrooms regime, but Gaertner (1965) assessed that a partial dryout occurs because the macrolayer is completely vapourised very quickly.

Iida and Kobayasi (1970) performed local void fraction measurements during boiling of water on a horizontal copper disk. These authors showed that, at low heat flux, a maximum of the void fraction ($\alpha \approx 70\%$) occurs about 2 mm above the surface, at the centre of the disk. At the periphery of the disk or in its immediate vicinity, the void fraction is low ($\alpha \approx 10\%$). So, the discrete bubbles generated on the whole surface tend to move towards the disk axis, probably drawn by

the wake of bigger vapour masses above the disk. At high heat flux, the void fraction reaches very high values ($\alpha \approx 95\%$) and decreases for increasing heights. This confirms the presence of large vapour masses observed by Gaertner (1965).

Some results, reported by Carvalho (1992) for boiling of FC-72 on a horizontal 5×5 mm^2 square heater simulating electronic chips have similar trends to those shown by Iida and Kobayasi (1970).

Liaw and Dhir (1989) measured void fraction profiles close to a vertical wall (6.3 cm wide and 10.3 cm high) during nucleate boiling of water using a γ-densitometer. They pointed out that, depending on the heat flux and the contact angle, the void fraction is nearly constant in the region close to the wall or reaches a maximum about 1–1.5 mm away from the wall. Thereafter it decreases nearly exponentially. They also emphasised that, even in the vicinity of the CHF, the void fraction is usually noticeably lower than 100%, ranging from 55% to 80%.

Carvalho (1992) investigated the two-phase flow structure during boiling of FC-72 at high heat flux in order to determine the triggering mechanisms of CHF. He pointed out the ability of hot-wire anemometry (HWA) to provide local information such as void fraction, bubble passage frequency, bubble passage time, which obviously gives a better insight into the structure of the flow than space-averaged void fraction measurements. Carvalho (1992) showed that the vapour is distributed along the width of the heated surface into "streamers" alternately with low and high void fraction. Because of the presence of the high void fraction streamers, the liquid flow towards the surface can be blocked, which results in a partial dryout and triggers the CHF.

From this brief literature review, we propose the following aims for this study:

- To clarify the dependence of the two-phase flow structure in the vicinity of a vertical wall, on which boiling takes place, through an experimental investigation. That will be obtained by means of HWA in order to get void fraction, bubble frequency, passage time and size.
- To determine objective criteria for the transitions between the regimes of nucleate boiling.

2. Experimental set-up

2.1. Experimental apparatus and procedure

The experimental apparatus (Fig. 2) and procedure have been described with many details in a previously published paper (Bonjour and Lallemand, 1998). It mainly consists of a gas- and liquid-tight vessel, including a transparent window so that visualisations can be performed, filled with saturated pentane. The test sample is a copper block (120 mm high and 60 mm wide) immersed in the liquid. It is heated by two electrical heaters (1000 W each) and, in order to reduce heat losses, it is thermally insulated on all its faces except on a vertical wall. The vapour generated on the surface rises up to the free interface and condenses in a water-cooled condenser. An auxiliary heater is used to keep the fluid at a fixed operating temperature independently of the power supplied to the copper block.

As regards instrumentation, a pressure gauge is used to measure the pressure (kept at 1 bar during all tests) in the vessel. A voltmeter and an ammeter allow the evaluation of the heat flux in the copper block. Thermocouples are used to measure the temperatures of the liquid, the vapour and at several locations in the test sample. The whole experimental procedure to obtain

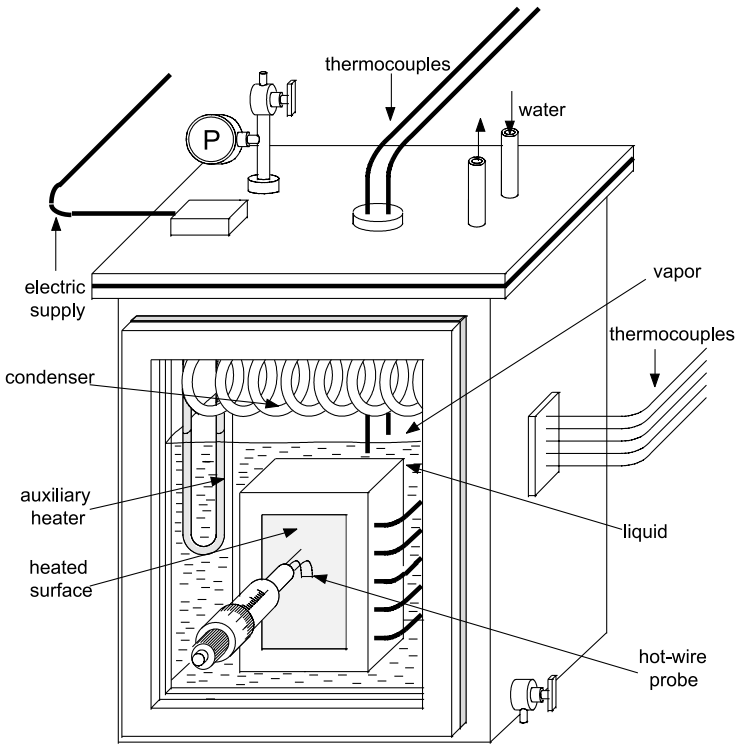

Fig. 2. Schematic diagram of the experimental apparatus.

reproducible boiling curves and CHF has been described in details previously by Bonjour and Lallemand (1995, 1997).

As suggested by Delhaye (1969), a hot-wire probe is used to achieve the phase detection and to measure the local characteristics of the two-phase flow near the heated wall. Its distance normal to the wall ranges from 0.1 to 18 mm and its location along the central vertical axis of the heated surface is variable. Since the minimum distance between the probe and the wall is 10 times lower than the typical diameter of isolated bubbles in the operating conditions (1 mm), measurements at the vicinity of the heated wall are thought to be a meaningful information on the bubble behaviour close to the wall. The same argumentation also applies to coalesced bubbles which are obviously bigger than isolated bubbles.

2.2. Hot-wire anemometry technique for phase detection

The equipment used for the HWA technique includes a constant temperature anemometer (CTA) model 1750 from TSI. A platinum coated tungsten wire (4 μm diameter and 0.125 mm long) is connected to the anemometer. The output signal of the anemometer is acquired by an acquisition card with a resolution of 5 mV and a conversion time of 25 μs. The sampling frequency is fixed to 2000 Hz and the sampling time to 6 s.

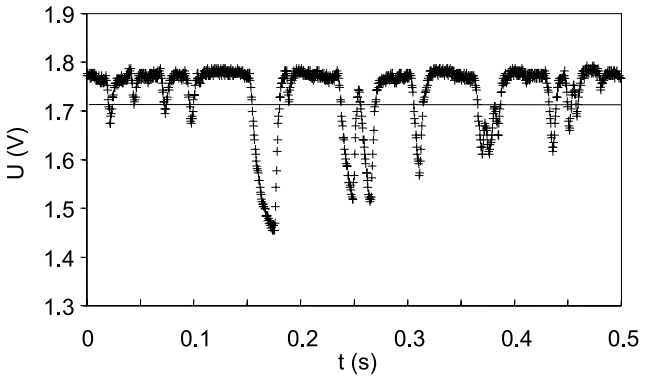

Fig. 3. Example of the anemometer output signal.

The anemometer mainly consists of a Wheatstone bridge, one leg of which is the hot-wire sensor. A secondary electronic circuit adjusts the voltage so that the hot-wire temperature is kept constant. Fig. 3 shows a typical evolution of the output signal as a function of time. When the sensor is in contact with liquid, the voltage is high because of the efficient cooling of the wire. During a void passage, the voltage drops rapidly because of the low heat transfer coefficient of the vapour.

Following the procedure proposed by Carvalho and Bergles (1991), we found (Bonjour, 1996) that the optimum sensor superheat is 68 K (i.e., a wire temperature of 104°C). For such a sensor superheat, boiling takes place very locally on the wire. The presence of bubbles on the wire result in high frequency oscillations of the voltage between the values $U = 1.74$ and 1.79 V (boiling noise) as shown in Fig. 3. Bubbles generated on the heated wall have a frequency of the order of 0–100 Hz and their diameter ranges from about 1 mm (isolated bubbles) to several centimetres (coalesced bubbles). So, they indubitably correspond to the large voltage variations and the boiling noise can be considered as negligible as referred to the anemometer output signal.

As regards the threshold, it was fixed to 1.71 V. So, in Fig. 3, each spike reaching a value lower than 1.71 V indicates a bubble passage. The beginning of a bubble passage is defined as the first point before a continuous decrease in the signal down to a voltage lower than 1.71 V. The end of the bubble passage corresponds to the last point after a continuous increase in the signal from a voltage lower than the threshold to a voltage greater than it. Owing to a data-reduction computer code, the local time-averaged void fraction, bubbles passage frequency and bubbles passage mean time are calculated from the following definitions:

$$\alpha = \frac{\Sigma t_{b,i}}{t_t}, \tag{1}$$

$$f_b = \frac{N}{t_t}, \tag{2}$$

$$t_b = \frac{\Sigma t_{b,i}}{N}, \tag{3}$$

where $t_{b,i}$ is the bubble passage time of the bubble number i, t_t the total sampling time and N the total number of bubble passages during t_t.

As regards the physical significance of the local time-average parameters measured by HWA, Carvalho (1992) mathematically demonstrated that the local time-average of the space fraction is equal to the instantaneous space-average of the local time-fraction. He also showed that because of the chaotic nature of boiling and under the ergodic hypothesis, the local time fraction can be properly measured from a single observed time history record.

3. Experimental results and discussion

The analysis of the experimental results is based on the following data:

- The void fraction profiles obtained from three vertical positions ($z = 20$, 60 and 100 mm) of the hot-wire sensor for various heat fluxes (Fig. 4). The bubble layer thickness, i.e., the abscissa for which the void fraction is equal to zero, increases with increasing heat flux and height.
- The frequency and time of bubble passages, plotted as a function of the reduced heat flux (ratio of the heat flux to the critical heat flux q'/q'_{crit}) in Figs. 5 and 6, respectively. For these measurements, the data acquisition was made at the same vertical locations as for the void fraction and 1.25 mm away from the wall.
- The contribution to the void fraction of three types of bubbles: short, average and long bubbles (Fig. 7) plotted vs. the reduced heat flux. The classification of bubbles based on their passage time follows a method proposed by Bonjour (1996) using the HWA technique to identify the flow patterns during boiling in a confined space. Long bubbles are bubbles whose duration is higher than 14 ms short bubbles less than 6 ms and average bubbles are between these transition values which were obtained from a study of the bubble passage time distribution. The contribution of a bubble category to the void fraction is defined as the ratio of the sum of the bubble passage times corresponding to this category to the sum of all the bubble passage times, so that it represents a percentage of the total void fraction. During measurements, the probe, facing the heated wall ($z = 60$ mm), was 1.25 mm away from it.

Three boiling behaviours, corresponding to three two-phase flow patterns are found.

3.1. High heat flux

At high heat flux ($q' = 23$ W/cm^2), whatever is the vertical location, the void fraction remains invariant at the vicinity of the heated wall ($y < 1.25$ mm for $z = 20$ mm to $y < 2.5$ mm for $z = 100$ mm) as can be seen in Fig. 4. This indicates that very large vapour masses (coalesced bubbles) are present. Even though it cannot be definitely be assessed if these bubbles slide along the wall or if they are still attached forming a dry patch, the former behaviour seems more likely to occur. Indeed, for very large bubbles, the buoyancy force is very important and tends to detach the bubbles. Moreover, even though the bubble passage time increases very sharply whereas the bubble frequency sharply decreases at high heat flux (Figs. 5 and 6), which might indicate that the vapour masses are stable on the wall, the void fraction never reaches 100% and the bubble frequency never completely drops down to zero. In other words, the vapour masses are much more stable on the wall than for the other ranges of heat flux, but they probably still have a rising motion close to the wall. These results suggest also that the high heat flux region corresponds to

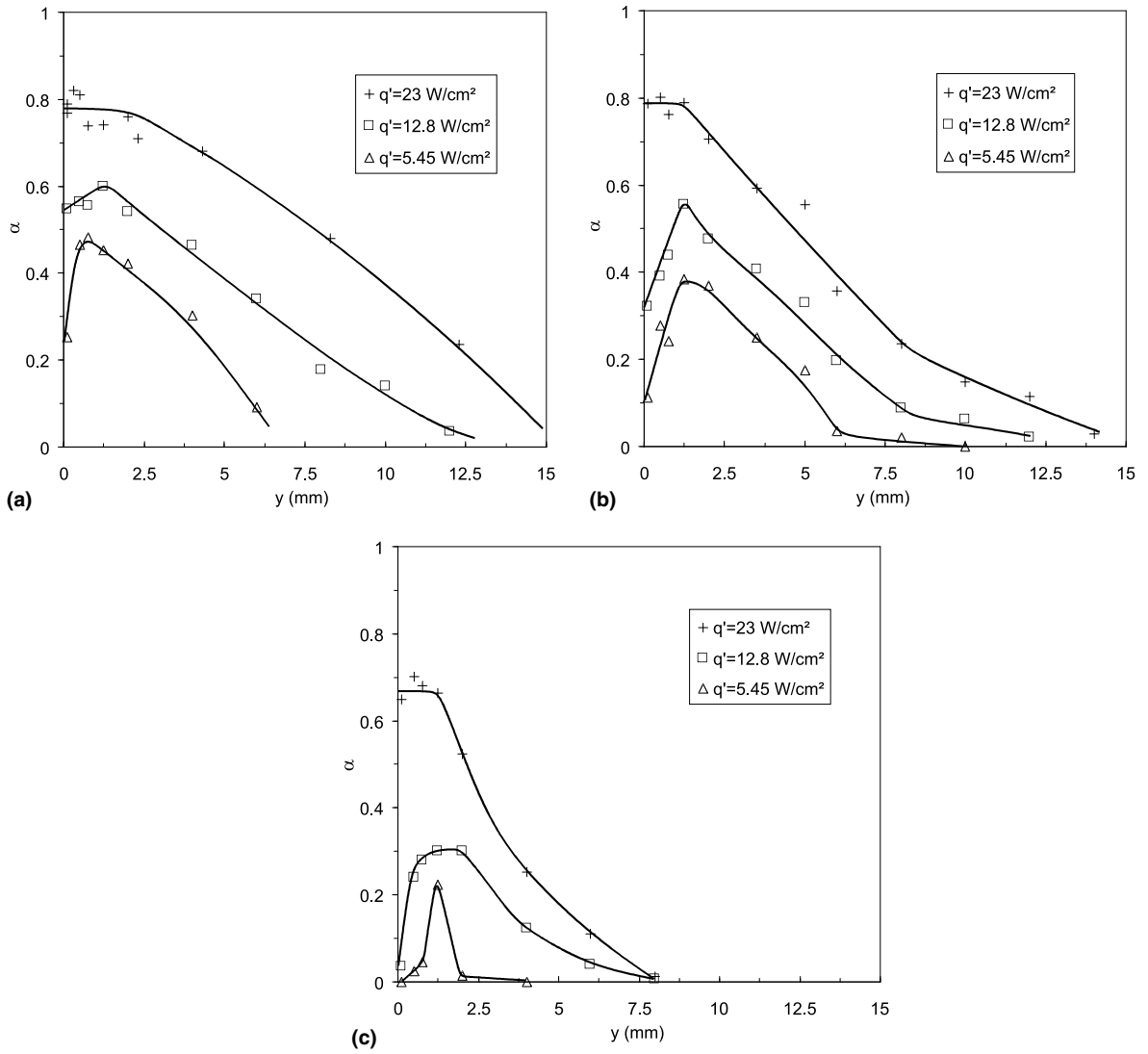

Fig. 4. Void fraction profile along the normal to the wall at various heights (100, 60 and 20 mm).

$q'/q'_{\mathrm{crit}} > 0.7$ and, from an analogy to Gaertner observation (1965), this flow pattern should be called *vicinity of CHF*. A schematic of this flow pattern is proposed in Fig. 8(a).

3.2. Low heat flux

For a low heat flux such as $q' = 5.45$ W/cm^2, the graphs in Fig. 4 exhibit a maximum of void fraction for a distance to the wall of about 1.25 mm. Since the typical size of pentane bubbles is about 0.8 mm, it must be concluded that bubbles generated on the wall tend to leave the wall mainly along its normal direction to reach a bubble column located 1.25 mm away from the

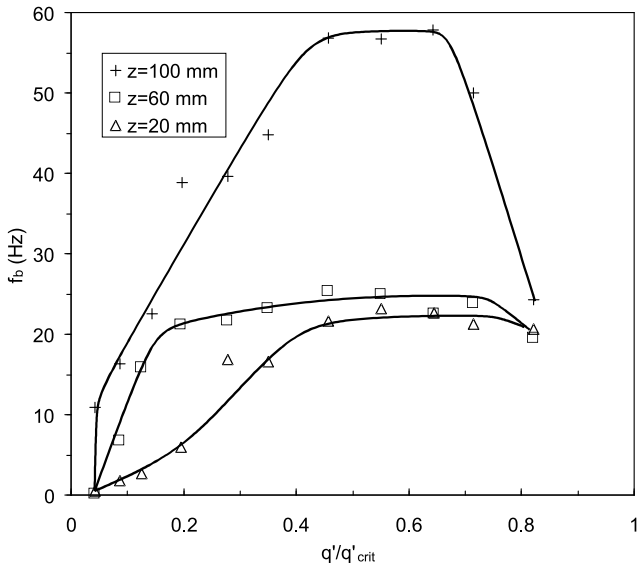

Fig. 5. Frequency of bubble passage.

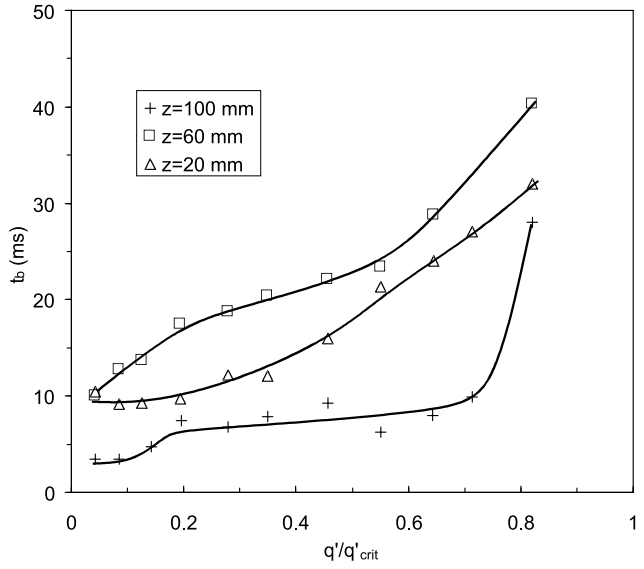

Fig. 6. Bubble mean passage time.

heated surface prior to adopting a rising motion in this column. Between the wall and the column or far from it, there are much fewer bubbles than in the column, which corresponds to the lower void fractions.

The normal detachment has been suggested by several authors. For example, Bibeau and Salcudean (1994) used a high-speed camera to study subcooled flow boiling of water and

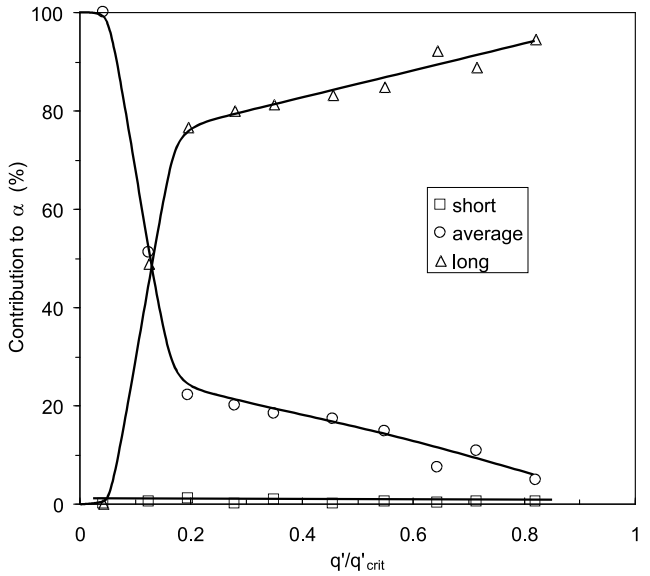

Fig. 7. Contribution of the various types of bubbles to the void fraction.

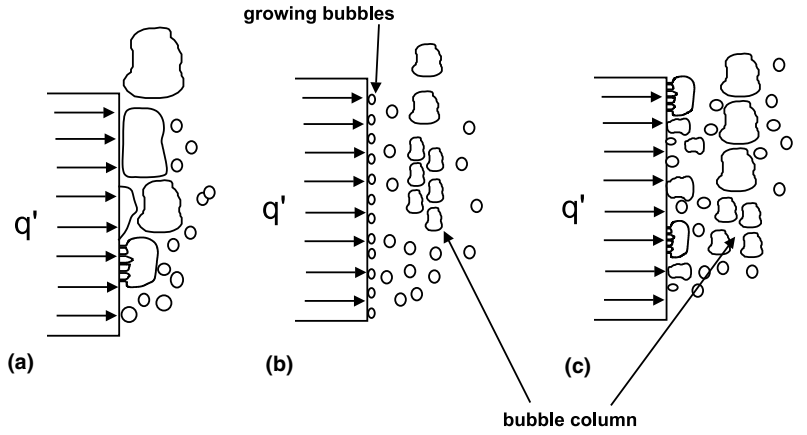

Fig. 8. Schematic of the two-phase flow structure for various heat fluxes: (a) high heat flux; (b) low heat flux; (c) moderate heat flux.

distinguished two types of bubble detachment, namely, a parallel detachment, which refers to a detachment when bubbles slide along the vertical wall, and a normal detachment, when bubbles are ejected from the wall into the bulk fluid. Parallel detachment occurs when the buoyancy force is predominant, which corresponds to large bubbles whereas normal detachment occurs when the surface tension force is the most important. Prodanovic et al. (1997) explained Bibeau and Salcudean (1994) observations when studying the forces acting on isolated bubbles during their growth and detachment. They showed that the surface tension forces are directed from the bubble to the wall during the bubble growth and from the bubble to the bulk fluid when bubbles leave the

wall, which facilitates the bubble detachment and tends to make the bubble move forward to the bubble column. However, the occurrence of normal or parallel detachment cannot be easily compared in this study with that of Bibeau and Salcudean (1994) and Prodanovic et al. (1997). Indeed, the effect of forced-convection greatly favours parallel detachment and, moreover, Prodanovic's model is linked to changes in the bubbles shape due to subcooled flow boiling particularities. Another relevant study was performed by Buyevich and Webbon (1996). They considered the behaviour of a bubble formed at an isolated nucleation site on a heated horizontal wall and showed that the surface tension force promotes the bubble detachment. Buyevich and Webbon (1997) suggested a dimensionless surface tension number, which, when being larger than unity, denotes that bubble detachment is mainly due to surface tension. Even though this criterion should probably be slightly modified for a vertical surface, its application for the operating conditions of the present study is believed to constitute a clue to determine the importance of the surface tension force in the bubble detachment. With the physical properties of pentane and moderate wall superheats (from 5 to 20 K) corresponding to low heat fluxes, the surface tension number is noticeably larger than unity, which leads to explain the formation of the bubble column to a certain distance away from the wall.

The profiles in Figs. 5 and 6 allow to reach a better understanding of the bubble behaviour in the bubble column. For low reduced heat fluxes, whatever is the position of the probe, the bubble passage time increases with increasing heat flux, which suggests an increase in the bubble diameter. As stated by Gaertner (1965), the frequency of bubble passages also increases with increasing heat flux. The bubble passage frequency increases with increasing height, which means that the distance between two successive bubbles decreases along the vertical axis. However, the bubble passage time is always greater for $z = 60$ mm than for $z = 20$ mm, but also for $z = 20$ mm than for $z = 100$ mm. This is due to the effect of two opposite phenomena. Indeed, on one hand, when bubbles rise from the lower part of the column to its upper part, they gather with bubbles generated on the upper part of the heated wall to form bubbles with larger diameters and consequently with larger passage times. On the other hand, their velocity is so increased during their rise along the vertical axis that, even with a large diameter in the upper part of the bubble column, their passage time is lower than in the medium region.

Fig. 7 is used to determine the end of the *isolated bubbles* flow pattern for low heat flux. The contribution of short bubbles to the void fraction is almost always zero. Indeed, in spite of the existence of very short bubbles ($t_{b,i} \approx 1$ ms), Fig. 6 shows that at low heat flux, the mean bubble passage time is about 10 ms. As regards average and long bubbles, two behaviours are observed in Fig. 7. For $q'/q'_{\mathrm{crit}} < 0.2$, there are almost only average bubbles whereas for $q'/q'_{\mathrm{crit}} > 0.2$, long bubbles are in the majority. This clearly indicates that the end of the isolated bubble flow pattern occurs for $q'/q'_{\mathrm{crit}} = 0.2$. This critical value of 0.2 for the reduced heat flux must be compared to the results of Nishikawa et al. (1974) that have been analysed by Dhir (1991). Indeed, it was shown by Dhir that for boiling of water on a vertical surface, the end of the regime called *partial nucleate boiling*, characterised by isolated bubbles at low heat flux took place for $q' = 20$ W/cm^2. Since the order of magnitude for the critical heat flux of boiling water is widely recognised to be 100 W/cm^2, this transition occurs for a reduced heat flux of about 0.2. This value also seems to be consistent with Gaertner's observations who found the transition for $q'/q'_{\mathrm{crit}} \approx 0.15$. However, the experimental conditions in these studies were very different from the present conditions and it can not be concluded that the transition value found in this study has a universal validity. The

schematic in Fig. 8(b) represents the isolated bubbles two phase flow described above, with small bubbles on the wall and the bubble column.

3.3. Moderate heat flux

As explained before, the moderate heat flux domain corresponds to reduced heat fluxes ranging from 0.2 to 0.7. For these conditions, a maximum in the void fraction occurs about 1.5 mm away from the heated wall, which, for the same reasons as for low heat fluxes, reveals the presence of a column in which bubbles preferably rise. The bubbles in the column coalesce during their rise since the contribution of long bubbles is higher than that of average bubbles. This flow structure is obviously comparable to that called *vapour mushrooms* by Gaertner (1965), but could also be called *fully developed nucleate boiling* following Dhir's classification (1991). The choice of the most appropriate name for that flow pattern should depend on if coalescence between neighbouring bubbles occurs on the heated wall, but unfortunately, this issue does not clearly appear from the experimental results. Lateral coalescence can seem likely to occur since, when increasing the heat flux, the number of active nucleation sites increases, which increases the probability for two neighbouring bubbles to coalesce. It has nevertheless been shown (Bonjour et al., 2000) that lateral coalescence does not always appear when the nucleation sites are close the ones to the others because the activation of a nucleation site sometimes makes its neighbours inactive due to a local heat flux deviation. Moreover, a theoretical analysis performed by Buyevich and Webbon (1997) concluded that the end of the isolated bubble regime is not due to coalescence between neighbouring bubbles but between successive bubbles. That is the reason why the schematic of the two-phase structure during the fully developed nucleate boiling regime (Fig. 8(c)) shows both laterally and longitudinally coalescing bubbles, since Dhir (1998) stated that these two types of coalescence occur approximately in the same time.

3.4. Comparison with reported experimental results

Since the previous works intending to describe the two-phase flow structure during boiling have been performed for many kinds of situations (wall orientation, fluid, influence of the contact angle etc...), few comparisons between experimental results have been made in the literature. In order to realise such comparisons, it is necessary to introduce dimensionless numbers. Fig. 9 shows the void fraction values at midplane of the heated wall measured by Liaw and Dhir (1989), Carvalho and Bergles (1991) and during the present experiments for almost identical reduced heat flux (q'/q'_{crit}) as a function of the dimensionless distance to the wall defined as:

$$y^+ = \frac{y}{\sqrt{\sigma/(g(\rho_\mathrm{l} - \rho_\mathrm{v}))}}, \tag{4}$$

where y is the distance to the wall, σ the surface tension, g the gravitational acceleration, ρ_l and ρ_v the liquid and vapour densities, respectively.

The characteristic length used in Eq. (4) has been widely used to represent the average bubble detachment diameter (Liaw and Dhir, 1989; Bonjour and Lallemand, 1995) so that if $y^+ > 1$, the point is supposed to be away from bubbles attached to the wall.

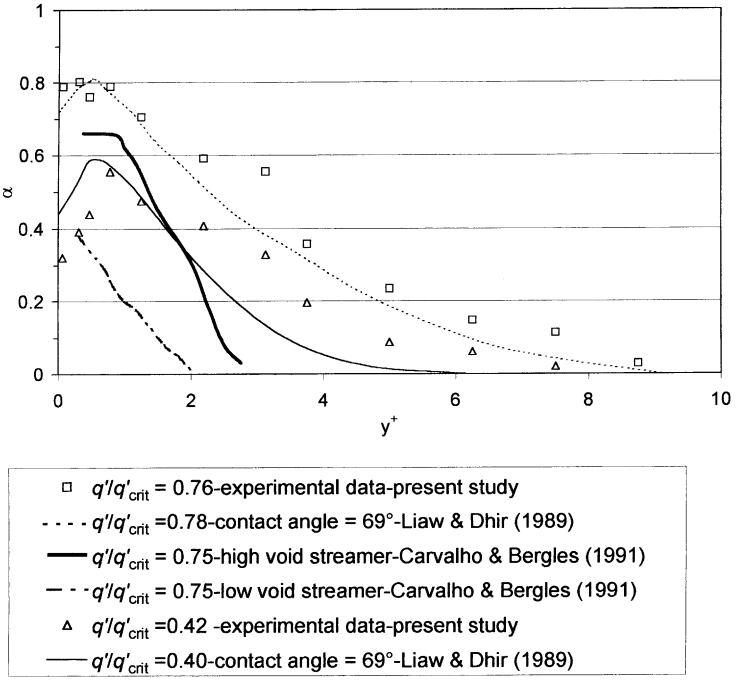

Fig. 9. Void fraction as a function of the reduced distance to the wall from the present data and those reported by Liaw and Dhir (1989) and Carvalho and Bergles (1991).

The results reported by Liaw and Dhir (1989) were obtained during water boiling on a vertical surface whose dimensions were similar to those of the wall used in the present investigation. However, these authors studied in detail the effect of the contact angle (varying from 14° to 90°) so that a typical contact angle value had to be chosen for the comparison (namely 69°).

As regards the results of Carvalho and Bergles (1991), they pointed out the presence of high and low void fraction streamers in the vicinity of the heated wall (a square heater with a side length of 5 mm). That is the reason why Fig. 9 shows the void fraction profiles for both streamers.

From this comparison, it appears that, when a maximum of the void fraction occurs, it is located at a dimensionless distance close to unity. Indeed, the void fraction is maximum because its measurement takes into account both the bubbles attached to the wall and the rising bubbles in the bubble column described in the previous sections.

The dimensionless profiles observed in the present study are in a reasonable agreement with those measured by Liaw and Dhir (1989), the difference being mainly attributed to the overall uncertainties. On the contrary, the present data are definitely different from those of Carvalho and Bergles (1991). It can consequently be thought that the heater size has a great effect on the void fraction profiles and that this effect is not enough taken into account by the chosen dimensionless parameters. The heater size effect is partially included in the reduced heat flux since a clear dependency of the critical heat flux on the heater dimensions has clearly been shown in the literature. Park and Bergles (1985) showed that for small heaters the CHF decreases as the height increases. However, when the heater is sufficiently tall, its height has no more influence on CHF. As regards

the heater width, these authors showed that CHF decreases as it increases. So, for sufficiently tall and wide heaters, CHF does not depend on the size and the reduced heat flux can be thought as being an appropriate dimensionless number to compare experimental results. However, for small heaters, the side effects become important and the boiling behaviour of fluids heated up to the same reduced heat flux will be noticeably different.

4. Conclusion

The two-phase flow structure during pool boiling of pentane on a vertical wall has been studied experimentally by means of hot wire anemometry. It has been pointed out that at low and moderate heat flux, i.e., for the flow patterns called *isolated bubbles* and *fully developed nucleate boiling,* respectively, when the bubbles leave the heated wall, they are ejected along the normal to the wall prior to rising in a bubble column located about 1.25 mm away from the wall. This is consistent with the theoretical studies of Prodanovic et al. (1997) and Buyevich and Webbon (1996), according to whom the surface tension forces promote a bubble normal detachment. On the contrary, at high heat flux (vicinity of CHF), the coalesced bubbles remain close to the wall during their rise. From the HWA measurements, criteria for the transition between the two-phase flow patterns have also been determined: the transition from *isolated bubbles* (or *partial nucleate boiling*) to *fully developed nucleate boiling* occurs for $q'/q'_{\mathrm{crit}} = 0.2$ and that from fully developed nucleate boiling to the vicinity of CHF for $q'/q'_{\mathrm{crit}} = 0.7$. These values should naturally be confirmed by further experiments under different conditions (different fluids, pressures, wall orientation, wall roughness, etc.) to establish the extension of their validity.

This work provides a useful framework for the development of a mechanistic model of pool boiling, which should constitute the next step of this study. The whole experimental results (time and frequency of bubble passages and void fraction) will be used to validate this model.

References

Bibeau, E.L., Salcudean, M., 1994. A study of bubble ebullition in forced-convective subcooled nucleate boiling at low pressure. Int. J. Heat Mass Transfer 37, 2245–2259.

Bonjour, J., 1996. Amélioration des transferts de chaleur enébullition naturelle convective par effet de confinement. Thèse de doctorat. INSA, Lyon, France.

Bonjour, J., Lallemand, M., 1995. Influence de la pression et du confinement sur les transferts thermiques au cours de l'ébullition convective naturelle. Rev. Gén. Therm. 34, 667–677.

Bonjour, J., Lallemand, M., 1997. Effects of confinement and pressure on critical heat flux during natural convective boiling in vertical channels. Int. Comm. Heat Mass Transfer 24, 191–200.

Bonjour, J., Lallemand, M., 1998. Flow patterns during boiling in a narrow space between two vertical surfaces. Int. J. Multiphase Flow 24, 947–960.

Bonjour, J., Clausse, M., Lallemand, M., 2000. Experimental study of the coalescence phenomenon during nucleate pool boiling. Exp. Therm. Fluid Sci. 20, 180–187.

Buyevich, Yu.A., Webbon, B.W., 1996. Dynamics of vapor bubbles in nucleate boiling. Int. J. Heat Mass Transfer 39, 2409–2426.

Buyevich, Yu.A., Webbon, B.W., 1997. The isolated bubble regime in pool nucleate boiling. Int. J. Heat Mass Transfer 40, 365–377.

Carvalho, R.D.M., Bergles, A.E., 1991. The use of hot-wire anemometry for local void fraction measurements in pool boiling. In: Proceedings of the 11th ABCM Mechanical Engineering Conference (XI COBEM), vol. 1, pp. 279–282.

Carvalho, R.D.M., 1992. The pool nucleate boiling and critical heat flux of vertically oriented, small heater boiling on one side. Ph.D. Thesis. RPI, Troy, NY.

Delhaye, J.M., 1969. Hot film anemometry in two-phase flow. In: Proceedings of the 11th National ASME/AIChE Heat Transfer Conference: Two-Phase Flow Instruments, pp. 58–69.

Dhir, V.K., 1998. Boiling Heat Transfer. Annu. Rev. Fluid Mech. 30, 365–401.

Dhir, V.K., 1991. Nucleate and transition boiling heat transfer under pool and external flow conditions. Int. J. Heat Fluid Flow 12, 290–314.

Gaertner, R.F., 1965. Photographic study of nucleate pool boiling on a horizontal surface. J. Heat Transfer 2, 17–29.

Iida, Y., Kobayasi, K., 1970. An experimental investigation on the mechanism of pool boiling phenomena by a probe method. In: Proceedings of the Fourth International Heat Transfer Conference, Versailles, France 5, paper B1.3.

Liaw, S.P., Dhir, V.K., 1989. Void fraction measurements during saturated pool boiling of water on partially wetted vertical surfaces. J. Heat Transfer 111, 731–738.

Nishikawa, K., Fujita, Y., Ohta, H., 1974. Effect of surface configuration on nucleate boiling heat transfer. Int. J. Heat Mass Transfer 27, 1559–1571.

Park, K.A., Bergles, A.E., 1985. Heat transfer characteristics of simulated microelectronic chips under normal and enhanced conditions. Technical report. College of Engineering Iowa State University, HTL-35, ERI Project 1544, ISU-ERI-Ames-86211, p. 183.

Prodanovic, V., Fraser, D., Salcudean, M., 1997. A study of forces acting on a single bubble in subcooled flow boiling at low pressure. In: Proceedings of the National Heat Transfer Conference, Baltimore, p. 12.